ORIGINAL PAPER

CrossMark

Method for Measuring Rock Mass Characteristics and Evaluating the Grouting-Reinforced Effect Based on Digital Drilling

Qi Wang[1,2] · Hongke Gao[1,2] · Hengchang Yu[1,2] · Bei Jiang[1,2,3] · Bohong Liu[1]

Abstract

Various types of broken rock masses, such as those in fault-fracture zones and fracture zones, which form as a result of disturbance from tunnelling, are often encountered during underground engineering construction. These rock masses have low self-supporting capacity and poor stability, which can easily cause damage to surrounding rock, such as large deformation features, collapse and falling blocks, etc., posing a threat to construction safety. During a field project, reinforcement by grouting is a primary means for addressing the aforementioned problems. The effective measurement of rock mass characteristics (e.g., rock layer interfaces and the broken area of surrounding rock) provides a basis for the reasonable design of a grouting scheme. The quantitative evaluation of the effect of rock mass grouting is essential for optimizing the grouting scheme. In view of this, in this study, a multi-functional rock mass digital drilling test system and a special polycrystalline diamond compact drill bit for digital testing were developed and were applied to conduct digital drilling tests on intact, broken and grouted rock masses. In addition, a digital drilling test (DDT) technique-based method for measuring rock mass characteristics in real time and rapidly evaluating the grouting effect was proposed. The proposed method is capable of identifying rock layer interfaces, determining the broken area and obtaining the equivalent strength of grouted rock masses. This method is advantageous for obtaining quantitative and rapid test results, which can provide a theoretical basis and technical means for optimizing the grouting parameters and designing support schemes for underground engineering construction.

List of symbols

V	Drilling rate
N	Rotational speed
M	Drilling torque
F	Drilling pressure
η_c	Cutting energy consumed by drill bit to cut a unit volume of rock
R_{uc}	Equivalent uniaxial compressive strength
S_i	No. of each test specimen
S_{ij}	No. of each layer of a test specimen
D_h	Drilling depth
t	Drilling time
W_M	Work done by M
W_F	Work done by F
E_c	Energy consumed to cut and crush the rock
E_f	Energy consumed by the friction between the drill bit and the bottom rock
R	Radius of the special drill bit
L_i	Length of the ith cutting edge
μ	Coefficient of friction between the cutting edges of the drill bit and the bottom rock
R_c	Uniaxial compressive strength of each rock layer of each rock specimen
δ_k	Ratio of the absolute value of the difference in η_c between an intact mass and a broken rock mass to the η_c for the same intact mass
η_{cw}	Amount of energy consumed by the drill bit to cut a unit volume of an intact rock mass
η_{cp}	Amount of energy consumed by the drill bit to cut a unit volume of a broken rock mass

✉ Qi Wang
chinawangqi@163.com

1 Research Center of Geotechnical and Structural Engineering, Shandong University, Jinan 250061, Shandong, China

2 Key Laboratory for Geo-mechanics and Deep Underground Engineering, China University of Mining and Technology, Beijing 100083, China

3 School of Civil Engineering and Architecture, University of Jinan, Jinan 250022, Shandong, China

δ_m Ratio of the absolute value of the difference in η_c between a grouted and a broken rock mass to the η_c for the same grouted rock mass

η_{cz} Amount of energy consumed by the drill bit to cut a unit volume of a grouted rock mass

1 Introduction

Various types of broken rock masses, such as those in fault-fracture zones (Bayati and Hamidi 2017; Dalgıç 2003; Shahidi and Vafaeian 2005) and fracture zones, which form as a result of disturbance from tunnelling (Perras and Diederichs 2016; Pardoen et al. 2016; Yang et al. 2014), are often encountered during underground construction. Generally, these rock masses have poor mechanical properties, have low self-supporting capacities, and are prone to cause damage to surrounding rock (large deformation features, collapses, falling blocks, etc.), posing a threat to construction safety. The macroscopic mechanical properties of broken rock masses can be improved by grouting reinforcement. In addition, the cohesion and internal friction angle of broken rock masses on the structural plane can also be increased by filling and cementing their fractured surfaces, thereby enhancing their overall stability and self-supporting capacity. At present, grouting has become a primary means for addressing the problems of low self-supporting capacity and poor stability that are associated with broken rock masses.

The effective measurement of rock mass characteristics (e.g., rock layer interfaces and the broken areas of surrounding rock) provides a basis for the reasonable design of grouting schemes for underground construction. Determination of pre- and post-grouting strength parameters of broken rock masses is essential for evaluating the effect of grouting and subsequently optimizing the grouting scheme. Common methods for measuring rock mass characteristics and evaluating the results of grouting mainly include the coring method, the acoustic sounding method and the ground-penetrating radar method. The coring method is relatively intuitive and accurate, but its process is relatively complex, requires a long period of time to complete, and is costly. In addition, it is difficult to obtain high-quality cores from broken surrounding rock. Acoustic sounding and ground-penetrating radar methods are indirect test methods. It is relatively difficult to use these two methods to quantitatively evaluate grouted rock mass strength. Therefore, there is a need to develop a rapid and reliable technique for determining rock mass characteristics and a method for evaluating the effect of grouting for underground construction to facilitate the accurate measurement of rock mass strength parameters, rock layer interfaces and the broken area of rock masses that are encountered during underground construction to realize timely optimization of grouting parameters and support schemes to ensure construction safety.

The digital drilling test (DDT) technique (Chen and Yue 2015; Gui et al. 2002; Kahraman et al. 2003; Suzuki et al. 1995; Yang et al. 2012; Yue et al. 2004) is an on-the-spot survey technique for accurately controlling and monitoring drilling parameters (e.g., drilling rate, V, rotational speed, N, drilling torque, M, and drilling pressure, F) during the drilling process. Studies have shown strong correlations between drilling parameters and rock mass strength (Huang and Wang 1997; Karasawa et al. 2002; Mostofi et al. 2011; Yaşar et al. 2011) and structural characteristics parameters (Akin and Karpuz 2008; Schunnesson 1996, 1998). The DDT technique provides a new means for measuring rock mass characteristics and evaluating the effect of grouting. The key to this technique lies in establishing the quantitative relationships between drilling parameters and rock mass strength parameters. However, currently, a lack of systematic research is restricting further development of the DDT technique in this field.

To address the aforementioned problems, in this study, a multi-functional rock mass digital drilling test system and a special polycrystalline diamond compact (PDC) drill bit for digital testing were developed and used to perform the digital drilling test on intact, broken and grouted rock masses. The drilling parameters (V, N, M and F) monitored during the digital drilling test were determined. In addition, the cutting energy consumed by this type of drill bit to cut a unit volume of rock, η_c, was also determined through energy analysis. Based on the test results, the response law of the drilling parameters to rock layer interfaces was analysed, and the drilling parameters for intact, broken and grouted rock masses were compared. The feasibility and effectiveness of the DDT technique in identifying rock layer interfaces, determining the broken area of surrounding rock and evaluating the effect of grouting were investigated. Furthermore, an equivalent uniaxial compressive strength, R_{uc}, prediction model (DPR model) for rock was established based on the drilling parameters. On this basis, a DDT technique-based method for measuring rock mass characteristics and evaluating the effect of grouting was proposed.

2 Digital Drilling Test on Layered Rock Masses

2.1 Test Equipment

To measure rock mass characteristics and evaluate the effect of grouting based on the DDT technique, a multi-functional rock mass digital drilling test system was developed, as shown in Fig. 1. This system is capable of providing a maximum M of 400 N·m, a maximum N of 400 r/min and a
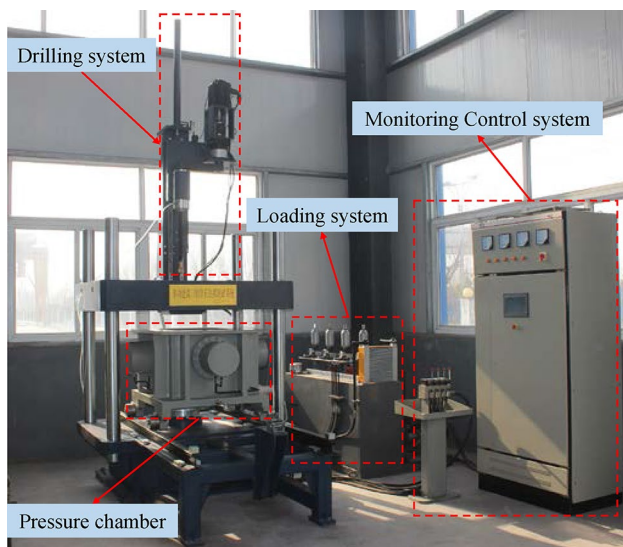
Fig. 1 The multi-functional rock mass digital drilling test system

maximum F of 50 kN and controlling and monitoring any of V, N, F and M and, thus, can be used to perform digital drilling tests of rock masses using various control modes.

2.2 Test Scheme Design

To establish the quantitative relationships between rock uniaxial compressive strength and drilling parameters, five layered test specimens were designed and produced. Each specimen consisted of three layers and included different combinations of an intact rock layer, a broken rock layer or a grouted rock layer. Each layer was lithologically composed of sandstone, limestone, mudstone or cement mortar. For each specimen, each of its layers was 100 mm in height with effective dimensions of 150 mm × 150 mm × 100 mm. In addition, a cement mortar was poured onto the external sides of each specimen to allow its layers to form a cube with dimensions of 300 mm × 300 mm × 300 mm. In this study, each test specimen was numbered using a combination of the letter S and a number; i.e., Si ($i = 1, 2, 3, 4, 5$). For example, S1 signifies the first specimen. Each layer of a test specimen is numbered using a combination of the number of the test specimen and another number; i.e., S_{ij} ($i = 1, 2, 3, 4, 5; j = 1, 2, 3$). For example, S12 signifies the second rock layer of the first specimen. Table 1 summarizes the preparation schemes for the layered rock specimens. The aggregates used to prepare broken and grouted rock masses of various lithologies had grain diameters between 20 and 30 mm. A cement grout with a water–cement ratio of 0.5, which is commonly used at construction sites, was used to prepare grouted rock masses. Table 2 summarizes the mix proportions for cement mortars with various strength grades.

Table 1 Scheme design for layered rock mass specimens for the digital drilling test

No.		Type of rock layer	No.		Type of rock layer
S1	S11	Intact limestone	S2	S21	M20 cement mortar
	S12	Broken mudstone		S22	Broken limestone
	S13	Intact sandstone		S23	Intact mudstone
S3	S31	M25 cement mortar	S4	S41	Grouted sandstone
	S32	Broken sandstone		S42	Grouted limestone
	S33	M10 cement mortar		S43	Grouted mudstone
S5	S51	M30 cement mortar			
	S52	M5 cement mortar			
	S53	M15 cement mortar			

In the test, the drilling modes, namely those controlling V and N and monitoring M and F were used. Figure 2 shows a layered rock mass specimen before and after a digital drilling test.

2.3 Statistics of the Test Results

A systematic test was conducted according to the test scheme. The drilling parameters (V, N, M and F) for each specimen were obtained. Based on the monitored values of the drilling parameters, the η_c associated with the special drill bit for digital drilling test was calculated through energy analysis and derivation.

2.3.1 Drilling Parameters Monitored During the Test

In the digital drilling test, V and N were set to 85 mm/min and 100 r/min, respectively. Here, the test data for specimen S1 are used as an example. Figure 3 shows the variation of the drilling depth D_h with the drilling time t during the drilling of specimen S1. Figures 4, 5 and 6 show the variation curves of N, M and F with D_h during the drilling of specimen S1, respectively.

Table 2 Mix proportions for cement mortars with various strength grades

Strength grades of cement mortar	Cement content (kg/m³)	Strength grades of cement	River sand content (kg/m³)	Water content (kg/m³)
M5	215	32.5	1450	300
M10	275			
M15	310			
M20	370	42.5		
M25	385			
M30	455			

Fig. 2 A layered rock mass specimen before and after a digital drilling test

Fig. 3 Variation curve of D_h with t during the drilling of specimen S1
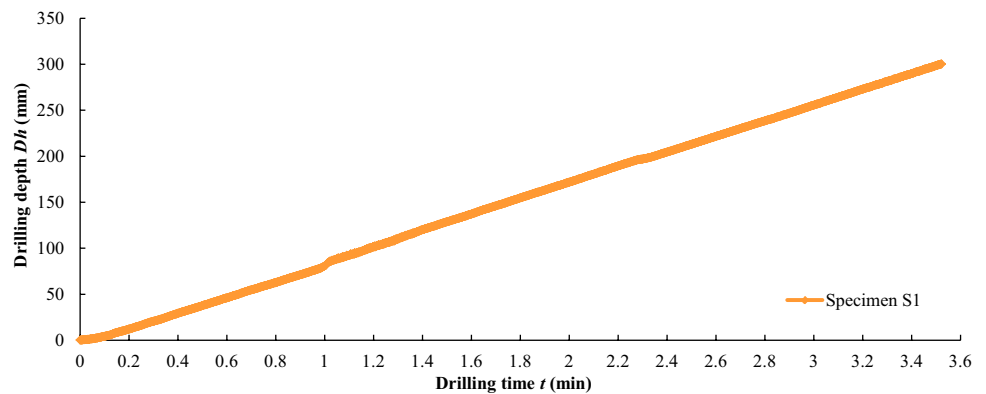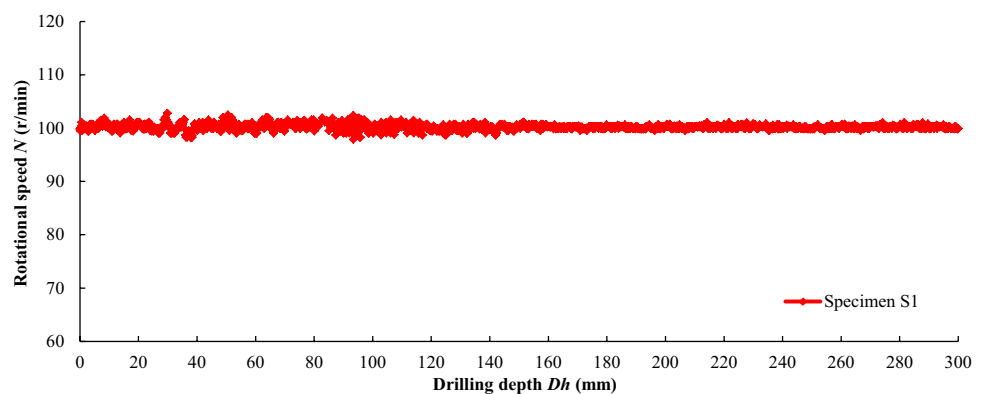

Fig. 4 Variation curve of N with D_h during the drilling of specimen S1

As demonstrated in Figs. 3 and 4, during the drilling of specimen S1, V ($V = D_h/t$, which was monitored by the sensor) remained close to the preset value of 85 mm/min, and N remained close to the preset value of 100 r/min, and the constant state was achieved.

Here, the S11 rock mass layer is used as an example for analysis. As demonstrated in Figs. 5 and 6, during the digital drilling test process, the variations of F and M with D_h exhibited a consistent law, which, overall, had two stages. (1) Increasing stage—before the drill bit came in contact with

the rock, F and M each had an initial value. After the drill bit came in contact with the rock, F and M increased rapidly as D_h increased within a relatively small range. (2) Stable stage—as D_h increased further, F and M gradually stabilized and fluctuated around their respective stable values.

Based on the previously mentioned variation patterns of F and M, test values for F and M were calculated by subtracting their respective initial values from their respective average values during the stable stage. Here, the measurements of M shown in Fig. 5 are used as an example. During

Fig. 5 Variation curve of M with D_h during the drilling of specimen S1
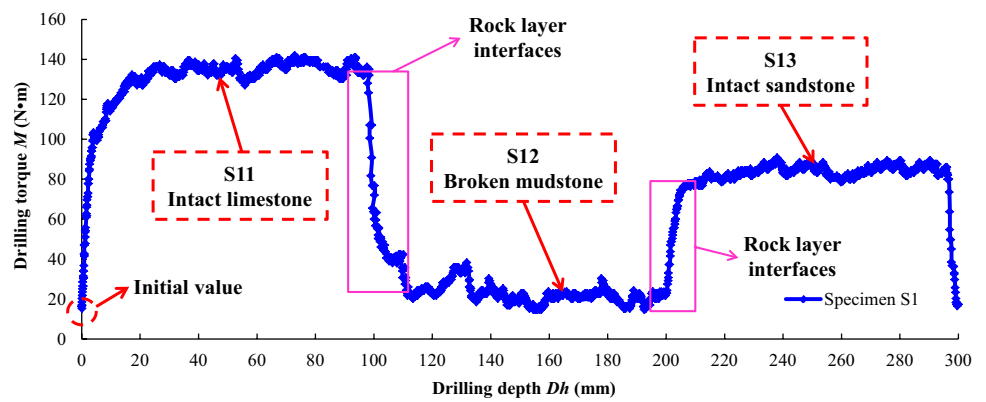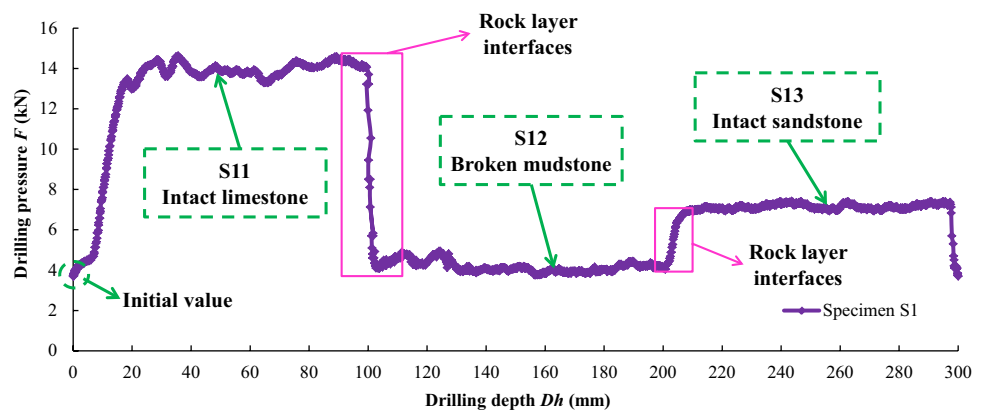

Fig. 6 Variation curve of F with D_h during the drilling of specimen S1

the drilling of specimen S1, the initial value of M, M_t, was 16.25 N·m; the M in the S11 layer, M_{11}, had an average value of 134.68 N·m during the stable stage; the M in the S12 layer, M_{12}, had an average value of 20.28 N·m during the stable stage; and the M in the S13 layer, M_{13}, had an average value of 87.04 N·m during the stable stage. Thus, the test value of the M in the S11 layer was calculated as follows: $M = M_{11} - M_t = 134.68 - 16.25$ N·m $= 118.43$ N·m; the test value of the M in the S12 layer was calculated as follows: $M = M_{12} - M_t = 20.28 - 16.25$ N·m $= 4.03$ N·m; and the test value of the M in the S13 layer was calculated as follows: $M = M_{13} - M_t = 87.04 - 16.25$ N·m $= 70.79$ N·m.

V, N, F and M in each rock layer monitored during the digital drilling test were calculated using the aforementioned drilling parameter calculation method. Table 3 summarizes the results.

2.3.2 η_c Determined Based on Energy Analysis

PDC drill bits are often used in rock drilling. A special PDC drill bit designed in-house for digital testing, as shown in Fig. 7, was used in the experiment. This special drill bit is composed of rectangular compacts and a matrix. The compacts are embedded in the matrix, forming three long cutting edges. Under the action of M and F, the drill bit drills the

specimens through rotation, and at the same time, the cutting edges cut and crush the rock, thereby forming a drill hole. The rectangular compact design prevents changes in the form and mechanical characteristics of the compacts during the drilling process, even if the compacts sustain wear, thus minimizing the effects of wear of the compacts on test data and facilitating establishment of an accurate mathematical model for the rock mass cutting process. Two main processes are involved in rock-cutting by the PDC through rotation: the cutting action of the cutting edges of the drill bit on the rock in front of it and the friction between the cutting edges and the rock at the bottom of it.

Teale (1965) proposed a parameter called the specific energy of drilling, η_s, which is defined as the amount of energy required to drill a unit volume of rock, which is given by:

$$\eta_s = \frac{F_s V_s + 2\pi N_s M_s}{\pi R_s^2 V_s} \tag{1}$$

where M_s is the torque on the drill bit; F_s is the driving force; N_s is the rotational speed; V_s is the drilling rate; and R_s is the radius of the drill bit.

η_s is related to rock properties (Karasawa et al. 2002; Tan et al. 2007) and is also affected by the performance

Table 3 Statistics of the digital drilling and uniaxial compression test results

| No.	V (mm/min)	N (r/min)	M (N m)	F (kN)	c (MPa)	R_c (MPa)
S_{11}	84.56	100.32	118.43	10.18	208.34	75.23
S_{12}	86.06	100.07	4.03	0.13	9.11	–
S_{13}	84.67	100.21	70.79	3.37	151.88	58.29
S_{21}	86.71	100.20	5.78	0.91	5.81	10.65
S_{22}	84.78	100.21	6.55	0.37	13.44	–
S_{23}	84.37	100.27	48.49	2.52	102.30	35.45
S_{31}	85.66	100.22	8.19	1.05	10.73	9.62
S_{32}	86.65	100.26	5.32	0.28	10.89	–
S_{33}	86.29	100.23	1.64	0.14	2.84	2.48
S_{41}	86.35	100.32	30.75	1.93	60.12	19.98
S_{42}	86.43	100.23	40.78	2.07	84.46	21.13
S_{43}	85.53	100.33	21.73	1.23	44.24	18.99
S_{51}	86.72	100.25	10.76	1.13	16.42	16.49
S_{52}	86.46	100.24	0.48	0.05	0.74	1.59
S_{53}	86.47	100.24	4.42	0.53	6.11	10.30
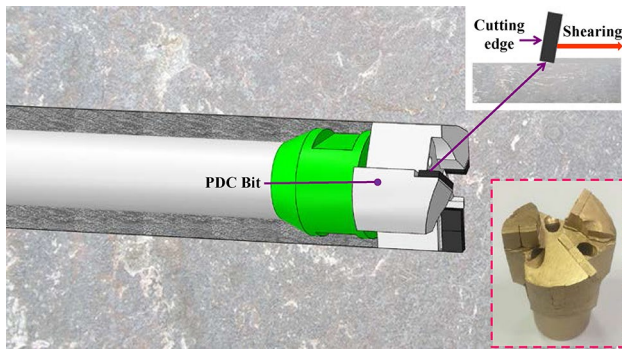
Fig. 7 The special PDC drill bit for digital drilling tests and the drill bit rock-cutting process
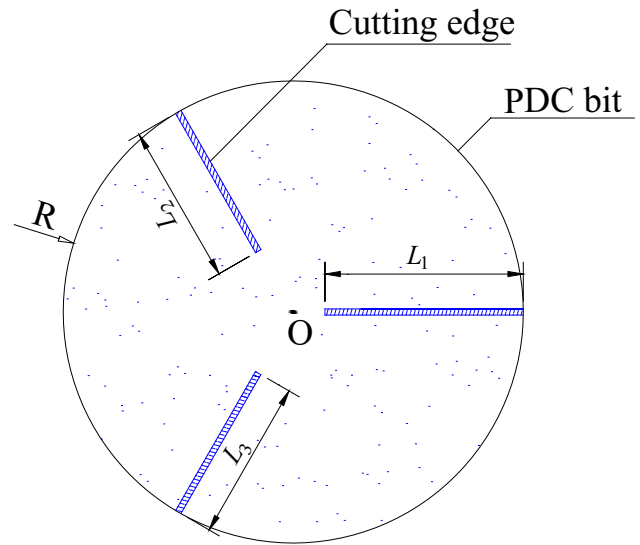

Fig. 8 A schematic diagram of the cutting edges of the special drill bit for digital drilling

of the drill bit and drilling parameters. This is because η_s describes the cutting action of the cutting edges of the drill bit on the rock combined with the friction between the cutting edges and the rock, whereas the friction between the drill bit and the rock at the bottom of it is determined by drilling parameters, including F.

The process in which the cutting edges of a drill bit cuts a rock is more closely related to rock properties than to friction. To eliminate the disturbance from friction, a new parameter, η_c, is defined in this study as the amount of energy consumed by the cutting edges of a drill bit to cut a unit volume of rock. The equation for calculating η_c is derived as follows:

Within a period of time t, the work done by a drilling machine to drill a rock includes the work done by M, W_M, and the work done by F, W_F, and the energy consumed during the drilling process includes the energy consumed to cut and crush the rock, E_c, and the energy consumed by

the friction between the drill bit and the bottom rock, E_f. According to the law of conservation of energy, we have

$$W_M + W_F = E_c + E_f \tag{2}$$

W_M is given by:

$$W_M = 2\pi NMt \tag{3}$$

W_F is given by:

$$W_F = FVt \tag{4}$$

As demonstrated in Fig. 8, the special drill bit for digital drilling has a radius of R and contains three cutting edges. The length of the ith cutting edge is L_i ($i = 1, 2, 3$). E_f is calculated as follows:

$$E_f = 2\pi N\mu t\left[\text{FR} - \frac{F(L_1^2 + L_2^2 + L_3^2)}{2(L_1 + L_2 + L_3)}\right], \quad (5)$$

where the specifications of the special drill bit for digital drilling are as follows: $R = 30$ mm, $L_1 = 27$ mm, $L_2 = 18$ mm and $L_3 = 18$ mm. In addition, μ is the coefficient of friction between the cutting edges of the drill bit and the bottom rock (μ is set as 0.21 based on the results of Yahiaoui et al. (2016)).

By substituting Eqs. (3), (4) and (5) into Eq. (2), E_c is obtained as follows:

$$E_c = 2\pi Nt\left[M - F\mu R + \frac{F\mu(L_1^2 + L_2^2 + L_3^2)}{2(L_1 + L_2 + L_3)}\right] + FVt, \quad (6)$$

where E_c is the amount of energy consumed to drill the rock during t. Thus, the η_c associated with the special drill bit for digital drilling is as follows:

$$\eta_c = \frac{2\pi NM - \pi\mu NF\left(2R - \frac{L_1^2 + L_2^2 + L_3^2}{L_1 + L_2 + L_3}\right) + FV}{\pi R^2 V} \quad (7)$$

By substituting the values of the aforementioned drilling parameters (V, N, M and F) monitored in each rock layer into Eq. (7), the η_c in each rock layer was determined. In addition, the uniaxial compression test was also performed to determine the uniaxial compressive strength, R_c, of each rock layer of each rock specimen. Table 3 summarizes the results.

3 Analysis of the Digital Drilling Test Results

3.1 Analysis of the Response of the Drilling Parameters to Rock Layer Interfaces

Surrounding rock structures of underground projects consist mostly of rock layers of various lithologies. Determining the locations of rock layers of various lithological compositions is an important step in a support scheme design. Herein, to realize the use of the DDT technique to identify rock layer interfaces, the response of the drilling parameters to rock layer interfaces is analysed with typical test data (the drilling parameters monitored during the drilling of specimen S1 (as shown in Figs. 5, 6) and the drilling parameters monitored during the drilling of specimen S5 (as shown in Figs. 9, 10).

An analysis of Figs. 5 and 6 shows that M and F have values of 118.43 N·m and 10.18 kN in the intact rock layer S11,

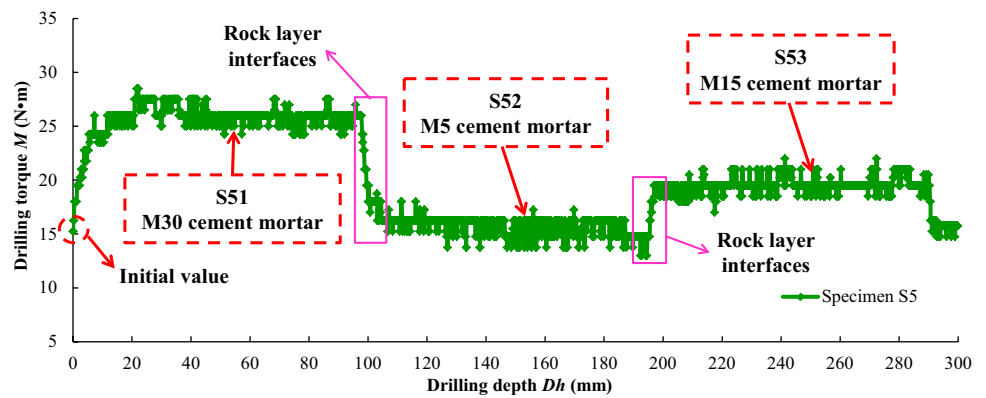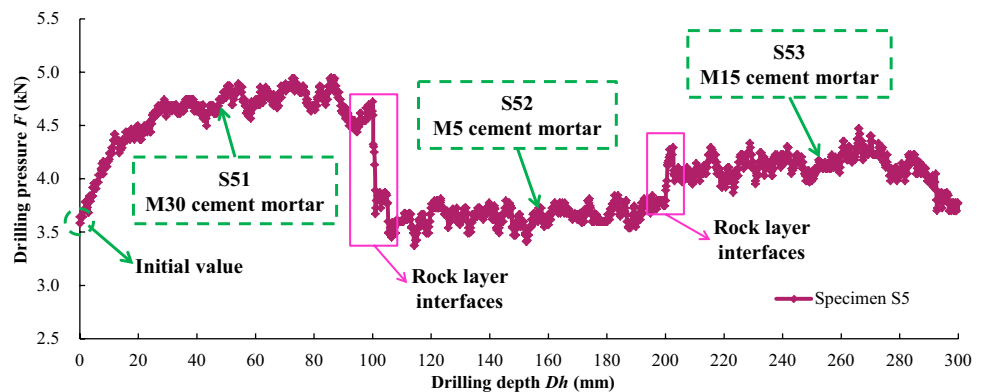**Fig. 9** Variation curve of M with D_h during the drilling of specimen S5

Fig. 10 Variation curve of F with D_h during the drilling of specimen S5

respectively, 4.03 N·m and 0.13 kN in the broken mudstone layer S12, respectively, and 70.79 N·m and 3.37 kN in the intact sandstone layer S13, respectively. Clearly, M and F varied significantly between the three rock layers, suggesting a relatively significant difference in rock mass strength. During the drilling process, as the drill bit entered layer S12 from layer S11, M and F decreased rapidly; as the drill bit entered layer S13 from layer S12, M and F increased rapidly. The response of the drilling parameters to interfaces between rock layers that varied significantly in strength was pronounced.

An analysis of Figs. 9 and 10 shows that M and F had values of 10.76 N·m and 1.13 kN in the M30-grade cement mortar layer S51, respectively, 0.48 N·m and 0.05 kN in the M5-grade cement mortar layer S52, respectively, and 4.42 N·m and 0.53 kN in the M15-grade cement mortar layer S53, respectively. Compared to specimen S1, there was a smaller difference in M and F and rock mass strength between the three rock layers of specimen S5. During the drilling process, as the drill bit entered layer S52 from layer S51, M and F decreased rapidly; as the drill bit entered layer S53 from layer S52, M and F increased rapidly. The response of the drilling parameters to interfaces between rock layers that differed insignificantly in strength was pronounced.

In summary, for specimen S1, the rock layers differed significantly in strength, and the difference in η_c between the rock layer with the highest strength (S11) and the rock layer with the lowest strength (S12) was 199.23 MPa. For specimen S5, the rock layers differed insignificantly in strength, and the difference in η_c between the rock layer with the highest strength (S51) and the rock layer with the lowest strength (S52) was 15.68 MPa. Clearly, the response of the drilling parameters to rock layer interfaces was relatively pronounced, regardless of how significant the difference in strength was between the rock layers. This validates the feasibility and effectiveness of the DDT technique in identifying rock layer interfaces.

3.2 Comparison of Drilling Parameters for Intact and Broken Rock Masses

The determination of the broken area of surrounding rock provides a basis for designing grouting schemes. To discuss the feasibility of the DDT technique in determining the broken area of surrounding rock, the drilling parameters for the digital drilling of intact and broken rock masses are compared, and an index δ_k that describes the ratio of the absolute value of the difference in η_c between an intact mass and a broken rock mass

to the η_c for an intact mass of the same rock is established, as shown in Eq. (8).

$$\delta_k = \frac{\left| \eta_{cw} - \eta_{cp} \right|}{\eta_{cw}} \times 100\%, \tag{8}$$

where η_{cw} is the amount of energy consumed by the drill bit to cut a unit volume of an intact rock mass and η_{cp} is the amount of energy consumed by the drill bit to cut a unit volume of the same broken rock mass.

Table 4 summarizes the calculated values of η_c for intact and broken limestone, sandstone and mudstone. Figure 11 compares the values of η_c for intact and broken rock masses of various lithologies.

An analysis of Table 4 and Fig. 11 shows that η_{cw} was significantly higher than η_{cp}. The δ_k for intact and broken limestone, sandstone and mudstone was 93.5%, 92.8% and 91.1%, respectively, and there was a significant difference between the response of η_c to the strength of an intact rock mass and a broken rock mass of the same lithology. This suggests that it is feasible and effective to use the DDT technique to determine the broken area of surrounding rock.

3.3 Comparison of the Drilling Parameters for Grouted and Broken Rock Masses

Currently, grouting is a primary means for addressing the low self-supporting capacity and poor stability problems associated with broken surrounding rock. A quantitative
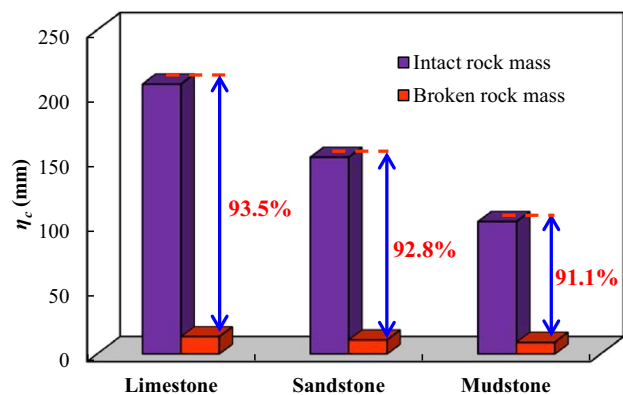

Fig. 11 Comparison of the η_c for digital drilling of intact and broken rock masses

Table 4 Summary of the calculated values of the drilling parameter η_c for digital drilling of intact and broken rock masses

No.	η_c (MPa)	No.	η_c (MPa)	No.	η_c (MPa)
S_{11} (intact limestone)	208.34	S_{13} (intact sandstone)	151.88	S_{23} (intact mudstone)	102.30
S_{22} (broken limestone)	13.44	S_{32} (broken sandstone)	10.89	S_{12} (broken mudstone)	9.11

Table 5 Summary of the calculated values of the drilling parameter η_c for digital drilling of grouted and broken rock masses

No.	η_c (MPa)	No.	η_c (MPa)	No.	η_c (MPa)
S_{22} (broken limestone)	13.44	S_{32} (broken sandstone)	10.89	S_{12} (broken mudstone)	9.11
S_{42} (grouted limestone)	84.46	S_{41} (grouted sandstone)	60.12	S_{43} (grouted mudstone)	44.24
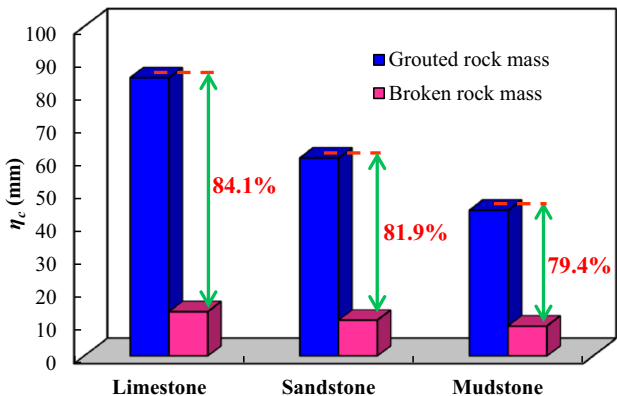
Fig. 12 Comparison of the η_c for digital drilling of grouted and broken rock masses

Fig. 13 Scatter diagram of the relationship between R_c and η_c

evaluation of the effect of grouting of rock masses is essential for optimizing a grouting scheme design. However, there are currently no effective methods for evaluating the effect of grouting. To discuss the feasibility of the DDT technique in evaluating the effect of grouting of rock masses, the values of the drilling parameter η_c for digital drilling of grouted and broken rock masses are compared, and an index δ_m that describes the ratio of the absolute value of the difference in η_c between a grouted and a broken rock mass to the η_c for the same grouted rock mass is established, as shown in Eq. (9).

$$\delta_m = \frac{|\eta_{cz} - \eta_{cp}|}{\eta_{cz}} \times 100\%, \tag{9}$$

where η_{cz} is the amount of energy consumed by the drill bit to cut a unit volume of a grouted rock mass and η_I is the amount of energy consumed by the drill bit to cut a unit volume of the same broken rock mass.

Table 5 summarizes the calculated values of η_I for grouted and broken limestone, sandstone and mudstone. Figure 12 shows the comparison of the values of η_I for grouted and broken rock masses of various lithologies.

An analysis of Table 5 and Fig. 12 shows that η_{cz} was significantly higher than η_{cp}. The δ_m for grouted and broken limestone, sandstone and mudstone was 84.1%, 81.9% and 79.4%, respectively, and the response of η_c to the strength of a broken rock mass differed significantly between before and after grouting. This validates the
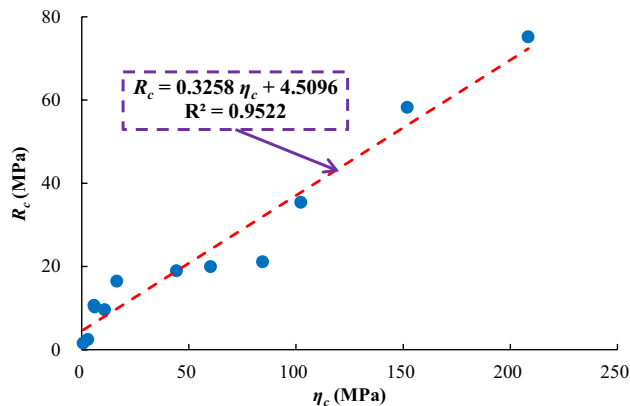
feasibility of the DDT technique in evaluating the effect of grouting for rock masses.

4 Digital Drilling-Based Determination of Rock Strength

4.1 An R_{uc} Prediction Model (DPR Model) for Rock

Figure 13 shows a scatter diagram of the relationship between η_c and R_c that was plotted based on the digital drilling test results for each rock layer that are shown in Table 3. An equation that describes the relationship between η_c and R_c is obtained by linear regression fit analysis. On this basis, an R_{uc} prediction model (DPR model) for rock is established.

An analysis of Fig. 13 shows a basically linear relationship between R_c and η_c. Overall, R_c increases as η_c increases. The rate of change of R_c with η_c is 0.3258. The goodness of fit R^2 is 0.9522, indicating a relatively good fit. Based on the optimum fitted curve for R_c and η_c, an equation that describes the relationship between η_c and R_c is obtained:

$$R_c = 0.3258\eta_c + 4.5096 \tag{10}$$

By substituting Eq. (7) into Eq. (10), an R_{uc} prediction model (DPR model) is obtained:

$$R_{uc} = 0.3258 \left[\frac{2\pi NM - \pi \mu NF(2R - \frac{L_1^2 + L_2^2 + L_3^2}{L_1 + L_2 + L_3}) + \text{FV}}{\pi R^2 V} \right] + 4.5096, \tag{11}$$

where the DPR model was obtained based on the digital drilling test results for a 12-layer rock mass with a strength ranging from 1.59 to 75.23 MPa. Digital drilling experiments on rock masses with a wider range of strengths will be performed to facilitate establishment of a DPR model with general applicability.

4.2 A Method for Measuring Rock Mass Characteristics and Evaluating the Effect of Grouting

Based on the aforementioned analysis, an on-the-spot method for measuring rock mass characteristics in real time and rapidly evaluating the effect of grouting for underground construction is proposed. The specific steps are as follows:

1. The digital drilling test system for surrounding rock is used to perform a digital drilling test on the rock mass in the field and obtain the drilling parameters (*V, N, M* and *F*) within the entire drilling area and in real time.
2. Based on the DPR model and the monitored drilling parameters, changes in R_{uc} with D_h within the entire drilling area are determined. On this basis, an R_{uc} distribution pattern for the surrounding rock is determined.
3. The obtained R_{uc} distribution pattern shows the locations where sudden changes in R_{uc} occur, i.e., the interfaces between rock masses that differ in strength. On this basis, the locations of the interfaces between rock layers, rock mass characteristics (e.g., broken areas) and equivalent strength of the rock mass are determined in real time.
4. If grouting is performed to reinforce the broken rock mass, based on the digital drilling test results and the DRP model, the distribution of R_{uc} before and after grouting can be determined. On this basis, the extent of increase in R_{uc} and the increase in the ratio of R_{uc} at the same depth after grouting can be determined, thereby achieving rapid evaluation of the reinforcing effect of grouting.
5. The R_{uc} distribution of rock obtained based on the digital drilling test results and the DPR model can provide basic data for designing and optimizing support schemes for underground engineering sites in a timely fashion.

5 Conclusions

1. A systematic comparison of digital drilling tests on intact, broken and grouted rock masses was conducted using a multi-functional rock masses digital drilling test system and a special PDC drill bit for digital test developed by authors. In addition, the η_c associated with this type of drill bit was also determined through energy analysis based on the values of drilling parameters that were monitored in real time.
2. The test results showed that the response of the drilling parameters for the digital drilling test to rock layer interfaces was pronounced and that the response of the drilling parameters to the strength of intact and broken rock masses differed significantly, thereby validating the feasibility and effectiveness of the DDT technique in identifying rock layer interfaces and measuring the broken areas of surrounding rock.
3. During the digital drilling test process, the response of the drilling parameter η_c to the strength of a broken rock mass differed significantly between before and after grouting. The values of δ_m are both higher than 75% for grouted and broken limestone, sandstone and mudstone. This validates the feasibility and effectiveness of the DDT technique in evaluating the effect of grouting for rock masses.
4. An R_{uc} prediction model (DPR model) based on the drilling parameters for the digital drilling test was established. A DDT technique-based method for measuring the rock mass characteristics in real time and rapidly evaluating the effect of grouting was proposed. This method is capable of identifying rock layer interfaces, determining the broken area and obtaining the strength of the grouted rock mass. In addition, digital drilling experiments on rock masses with a wider range of strengths will be carried out to construct a generally applicable DPR model, thereby realizing accurate, real time and rapid acquisition of the R_{uc} of surrounding rock during underground engineering construction based on the DDT technique and providing a theoretical basis and technical means for designing and optimizing support schemes for underground engineering construction in a timely fashion.

References

Akin S, Karpuz C (2008) Estimating drilling parameters for diamond bit drilling operations using artificial neural networks. Int J Geomech 8(1):68–73

Bayati M, Hamidi JK (2017) A case study on TBM tunnelling in fault zones and lessons learned from ground improvement. Tunn Undergr Space Technol 63:162–170

Chen J, Yue ZQ (2015) Ground characterization using breaking-action-based zoning analysis of rotary-percussive instrumented drilling. Int J Rock Mech Min Sci 75:33–43

Dalgıç S (2003) Tunneling in fault zones, Tuzla tunnel, Turkey. Tunn Undergr Space Technol 18(5):453–465

Gui MW, Soga K, Bolton MD, Hamelin JP (2002) Instrumented borehole drilling for subsurface investigation. J Geotech Geoenviron Eng 128(4):283–291

Huang SL, Wang ZW (1997) The mechanics of diamond core drilling of rocks. Int J Rock Mech Min Sci 34(3–4):134.e1-134.e14

Kahraman S, Bilgin N, Feridunoglu C (2003) Dominant rock properties affecting the penetration rate of percussive drills. Int J Rock Mech Min Sci 40(5):711–723

Karasawa H, Ohno T, Kosugi M, Rowley JC (2002) Methods to estimate the rock strength and tooth wear while drilling with rollerbits. J Energy Resour Technol 124(3):125–132

Mostofi M, Rasouli V, Mawuli E (2011) An estimation of rock strength using a drilling performance model: a case study in Blacktip field, Australia. Rock Mech Rock Eng 44(3):305–316

Pardoen B, Talandier J, Collin F (2016) Permeability evolution and water transfer in the excavation damaged zone of a ventilated gallery. Int J Rock Mech Min Sci 85:192–208

Perras MA, Diederichs MS (2016) Predicting excavation damage zone depths in brittle rocks. J Rock Mech Geo Eng 8(1):60–74

Schunnesson H (1996) RQD predictions based on drill performance parameters. Tunn Undergr Space Technol 11(3):345–351

Schunnesson H (1998) Rock characteristics using percussive drilling. Int J Rock Mech Min Sci 35(6):711–725

Shahidi AR, Vafaeian M (2005) Analysis of longitudinal profile of the tunnels in the active faulted zone and designing the flexible lining. Tunn Undergr Space Technol 20(3):213–221

Suzuki Y, Sasao H, Nishi K, Takesue K (1995) Ground exploration system using seismic cone and rotary percussion drill. J Arch Bui Sci 1(1):180–184

Tan ZY, Yue ZQ, Tan GH, Li CF (2007) Study on specific energy of diamond drilling and real-time classification of weathered granite. Chin J Rock Mech Eng 26(S1):2907–2912 **(in Chinese)**

Teale R (1965) The concept of specific energy in rock drilling. Int J Rock Mech Min Sci Geo Abs 2(1):57–73

Yahiaoui M, Paris JY, Delbé K, Denape J, Gerbaud L, Dourfaye A (2016) Independent analyses of cutting and friction forces applied on a single polycrystalline diamond compact cutter. Int J Rock Mech Min Sci 85:20–26

Yang WW, Yue ZQ, Tham LG (2012) Automatic monitoring of inserting or retrieving SPT sampler in drillhole. Geotech Test J 35(3):420–436

Yang HQ, Zeng YY, Lan YF, Zhou XP (2014) Analysis of the excavation damaged zone around a tunnel accounting for geostress and unloading. Int J Rock Mech Min Sci 69:59–66

Yaşar E, Ranjith PG, Viete DR (2011) An experimental investigation into the drilling and physico-mechanical properties of a rock-like brittle material. J Petrol Sci Eng 76(3):185–193

Yue ZQ, Lee CF, Law KT, Tham LG (2004) Automatic monitoring of rotary-percussive drilling for ground characterization—illustrated by a case example in Hong Kong. Int J Rock Mech Min Sci 41(4):573–612